ISSN 1726-5479

SENSORS & TRANSDUCERS

11/08 vol. 98

Nanosensors and Nanodevices

International Frequency Sensor Association Publishing

Sensors & Transducers

Volume 98
Issue 11
November 2008

www.sensorsportal.com

ISSN 1726-5479

Editor-in-Chief: professor Sergey Y. Yurish, phone: +34 696067716, fax: +34 93 4011989,
e-mail: editor@sensorsportal.com

Editors for Western Europe
Meijer, Gerard C.M., Delft University of Technology, The Netherlands
Ferrari, Vittorio, Universitá di Brescia, Italy

Editors for North America
Datskos, Panos G., Oak Ridge National Laboratory, USA
Fabien, J. Josse, Marquette University, USA
Katz, Evgeny, Clarkson University, USA

Editor South America
Costa-Felix, Rodrigo, Inmetro, Brazil

Editor for Eastern Europe
Sachenko, Anatoly, Ternopil State Economic University, Ukraine

Editor for Asia
Ohyama, Shinji, Tokyo Institute of Technology, Japan

Editorial Advisory Board

Abdul Rahim, Ruzairi, Universiti Teknologi, Malaysia
Ahmad, Mohd Noor, Nothern University of Engineering, Malaysia
Annamalai, Karthigeyan, National Institute of Advanced Industrial Science and Technology, Japan
Arcega, Francisco, University of Zaragoza, Spain
Arguel, Philippe, CNRS, France
Ahn, Jae-Pyoung, Korea Institute of Science and Technology, Korea
Arndt, Michael, Robert Bosch GmbH, Germany
Ascoli, Giorgio, George Mason University, USA
Atalay, Selcuk, Inonu University, Turkey
Atghiaee, Ahmad, University of Tehran, Iran
Augutis, Vygantas, Kaunas University of Technology, Lithuania
Avachit, Patil Lalchand, North Maharashtra University, India
Ayesh, Aladdin, De Montfort University, UK
Bahreyni, Behraad, University of Manitoba, Canada
Baoxian, Ye, Zhengzhou University, China
Barford, Lee, Agilent Laboratories, USA
Barlingay, Ravindra, RF Arrays Systems, India
Basu, Sukumar, Jadavpur University, India
Beck, Stephen, University of Sheffield, UK
Ben Bouzid, Sihem, Institut National de Recherche Scientifique, Tunisia
Benachaiba, Chellali, Universitaire de Bechar, Algeria
Binnie, T. David, Napier University, UK
Bischoff, Gerlinde, Inst. Analytical Chemistry, Germany
Bodas, Dhananjay, IMTEK, Germany
Borges Carval, Nuno, Universidade de Aveiro, Portugal
Bousbia-Salah, Mounir, University of Annaba, Algeria
Bouvet, Marcel, CNRS – UPMC, France
Brudzewski, Kazimierz, Warsaw University of Technology, Poland
Cai, Chenxin, Nanjing Normal University, China
Cai, Qingyun, Hunan University, China
Campanella, Luigi, University La Sapienza, Italy
Carvalho, Vitor, Minho University, Portugal
Cecelja, Franjo, Brunel University, London, UK
Cerda Belmonte, Judith, Imperial College London, UK
Chakrabarty, Chandan Kumar, Universiti Tenaga Nasional, Malaysia
Chakravorty, Dipankar, Association for the Cultivation of Science, India
Changhai, Ru, Harbin Engineering University, China
Chaudhari, Gajanan, Shri Shivaji Science College, India
Chen, Jiming, Zhejiang University, China
Chen, Rongshun, National Tsing Hua University, Taiwan
Cheng, Kuo-Sheng, National Cheng Kung University, Taiwan
Chiriac, Horia, National Institute of Research and Development, Romania
Chowdhuri, Arijit, University of Delhi, India
Chung, Wen-Yaw, Chung Yuan Christian University, Taiwan
Corres, Jesus, Universidad Publica de Navarra, Spain
Cortes, Camilo A., Universidad Nacional de Colombia, Colombia
Courtois, Christian, Universite de Valenciennes, France
Cusano, Andrea, University of Sannio, Italy
D'Amico, Arnaldo, Università di Tor Vergata, Italy
De Stefano, Luca, Institute for Microelectronics and Microsystem, Italy
Deshmukh, Kiran, Shri Shivaji Mahavidyalaya, Barshi, India
Dickert, Franz L., Vienna University, Austria
Dieguez, Angel, University of Barcelona, Spain
Dimitropoulos, Panos, University of Thessaly, Greece
Ding Jian, Ning, Jiangsu University, China
Djordjevich, Alexandar, City University of Hong Kong, Hong Kong
Ko, Sang Choon, Electronics and Telecommunications Research Institute,
Donato, Nicola, University of Messina, Italy
Donato, Patricio, Universidad de Mar del Plata, Argentina
Dong, Feng, Tianjin University, China
Drljaca, Predrag, Instersema Sensoric SA, Switzerland
Dubey, Venketesh, Bournemouth University, UK
Enderle, Stefan, University of Ulm and KTB Mechatronics GmbH, Germany
Erdem, Gursan K. Arzum, Ege University, Turkey
Erkmen, Aydan M., Middle East Technical University, Turkey
Estelle, Patrice, Insa Rennes, France
Estrada, Horacio, University of North Carolina, USA
Faiz, Adil, INSA Lyon, France
Fericean, Sorin, Balluff GmbH, Germany
Fernandes, Joana M., University of Porto, Portugal
Francioso, Luca, CNR-IMM Institute for Microelectronics and Microsystems, Italy
Francis, Laurent, University Catholique de Louvain, Belgium
Fu, Weiling, South-Western Hospital, Chongqing, China
Gaura, Elena, Coventry University, UK
Geng, Yanfeng, China University of Petroleum, China
Gole, James, Georgia Institute of Technology, USA
Gong, Hao, National University of Singapore, Singapore
Gonzalez de la Rosa, Juan Jose, University of Cadiz, Spain
Granel, Annette, Goteborg University, Sweden
Graff, Mason, The University of Texas at Arlington, USA
Guan, Shan, Eastman Kodak, USA
Guillet, Bruno, University of Caen, France
Guo, Zhen, New Jersey Institute of Technology, USA
Gupta, Narendra Kumar, Napier University, UK
Hadjiloucas, Sillas, The University of Reading, UK
Hashsham, Syed, Michigan State University, USA
Hernandez, Alvaro, University of Alcala, Spain
Hernandez, Wilmar, Universidad Politecnica de Madrid, Spain
Homentcovschi, Dorel, SUNY Binghamton, USA
Horstman, Tom, U.S. Automation Group, LLC, USA
Hsiai, Tzung (John), University of Southern California, USA
Huang, Jeng-Sheng, Chung Yuan Christian University, Taiwan
Huang, Star, National Tsing Hua University, Taiwan
Huang, Wei, PSG Design Center, USA
Hui, David, University of New Orleans, USA
Jaffrezic-Renault, Nicole, Ecole Centrale de Lyon, France
Jaime Calvo-Galleg, Jaime, Universidad de Salamanca, Spain
James, Daniel, Griffith University, Australia
Janting, Jakob, DELTA Danish Electronics, Denmark
Jiang, Liudi, University of Southampton, UK
Jiang, Wei, University of Virginia, USA
Jiao, Zheng, Shanghai University, China
John, Joachim, IMEC, Belgium
Kalach, Andrew, Voronezh Institute of Ministry of Interior, Russia
Kang, Moonho, Sunmoon University, Korea South
Kaniusas, Eugenijus, Vienna University of Technology, Austria
Katake, Anup, Texas A&M University, USA
Kausel, Wilfried, University of Music, Vienna, Austria
Kavasoglu, Nese, Mugla University, Turkey
Ke, Cathy, Tyndall National Institute, Ireland
Khan, Asif, Aligarh Muslim University, Aligarh, India
Kim, Min Young, Koh Young Technology, Inc., Korea South
Sandacci, Serghei, Sensor Technology Ltd., UK

Korea South
Kockar, Hakan, Balikesir University, Turkey
Kotulska, Malgorzata, Wroclaw University of Technology, Poland
Kratz, Henrik, Uppsala University, Sweden
Kumar, Arun, University of South Florida, USA
Kumar, Subodh, National Physical Laboratory, India
Kung, Chih-Hsien, Chang-Jung Christian University, Taiwan
Lacnjevac, Caslav, University of Belgrade, Serbia
Lay-Ekuakille, Aime, University of Lecce, Italy
Lee, Jang Myung, Pusan National University, Korea South
Lee, Jun Su, Amkor Technology, Inc. South Korea
Lei, Hua, National Starch and Chemical Company, USA
Li, Genxi, Nanjing University, China
Li, Hui, Shanghai Jiaotong University, China
Li, Xian-Fang, Central South University, China
Liang, Yuanchang, University of Washington, USA
Liawruangrath, Saisunee, Chiang Mai University, Thailand
Liew, Kim Meow, City University of Hong Kong, Hong Kong
Lin, Hermann, National Kaohsiung University, Taiwan
Lin, Paul, Cleveland State University, USA
Linderholm, Pontus, EPFL - Microsystems Laboratory, Switzerland
Liu, Aihua, University of Oklahoma, USA
Liu Changgeng, Louisiana State University, USA
Liu, Cheng-Hsien, National Tsing Hua University, Taiwan
Liu, Songqin, Southeast University, China
Lodeiro, Carlos, Universidade NOVA de Lisboa, Portugal
Lorenzo, Maria Encarnacio, Universidad Autonoma de Madrid, Spain
Lukaszewicz, Jerzy Pawel, Nicholas Copernicus University, Poland
Ma, Zhanfang, Northeast Normal University, China
Majstorovic, Vidosav, University of Belgrade, Serbia
Marquez, Alfredo, Centro de Investigacion en Materiales Avanzados, Mexico
Matay, Ladislav, Slovak Academy of Sciences, Slovakia
Mathur, Prafull, National Physical Laboratory, India
Maurya, D.K., Institute of Materials Research and Engineering, Singapore
Mekid, Samir, University of Manchester, UK
Melnyk, Ivan, Photon Control Inc., Canada
Mendes, Paulo, University of Minho, Portugal
Mennell, Julie, Northumbria University, UK
Mi, Bin, Boston Scientific Corporation, USA
Minas, Graca, University of Minho, Portugal
Moghavvemi, Mahmoud, University of Malaya, Malaysia
Mohammadi, Mohammad-Reza, University of Cambridge, UK
Molina Flores, Esteban, Benemérita Universidad Autónoma de Puebla, Mexico
Moradi, Majid, University of Kerman, Iran
Morello, Rosario, DIMET, University "Mediterranea" of Reggio Calabria, Italy
Mounir, Ben Ali, University of Sousse, Tunisia
Mukhopadhyay, Subhas, Massey University, New Zealand
Neelamegam, Periasamy, Sastra Deemed University, India
Neshkova, Milka, Bulgarian Academy of Sciences, Bulgaria
Oberhammer, Joachim, Royal Institute of Technology, Sweden
Ould Lahoucin, University of Guelma, Algeria
Pamidighanta, Sayanu, Bharat Electronics Limited (BEL), India
Pan, Jisheng, Institute of Materials Research & Engineering, Singapore
Park, Joon-Shik, Korea Electronics Technology Institute, Korea South
Penza, Michele, ENEA C.R., Italy
Pereira, Jose Miguel, Instituto Politecnico de Setebal, Portugal
Petsev, Dimiter, University of New Mexico, USA
Pogacnik, Lea, University of Ljubljana, Slovenia
Post, Michael, National Research Council, Canada
Prance, Robert, University of Sussex, UK
Prasad, Ambika, Gulbarga University, India
Prateepasen, Asa, Kingmoungut's University of Technology, Thailand
Pullini, Daniele, Centro Ricerche FIAT, Italy
Pumera, Martin, National Institute for Materials Science, Japan
Radhakrishnan, S. National Chemical Laboratory, Pune, India
Rajanna, K., Indian Institute of Science, India
Ramadan, Qasem, Institute of Microelectronics, Singapore
Rao, Basuthkar, Tata Inst. of Fundamental Research, India
Raoof, Kosai, Joseph Fourier University of Grenoble, France
Reig, Candid, University of Valencia, Spain
Restivo, Maria Teresa, University of Porto, Portugal
Robert, Michel, University Henri Poincare, France
Rezazadeh, Ghader, Urmia University, Iran
Royo, Santiago, Universitat Politecnica de Catalunya, Spain
Rodriguez, Angel, Universidad Politecnica de Cataluna, Spain
Rothberg, Steve, Loughborough University, UK
Sadana, Ajit, University of Mississippi, USA
Sadeghian Marnani, Hamed, TU Delft, The Netherlands
Sapozhnikova, Ksenia, D.I.Mendeleyev Institute for Metrology, Russia
Saxena, Vibha, Bhbha Atomic Research Centre, Mumbai, India
Schneider, John K., Ultra-Scan Corporation, USA
Seif, Selemani, Alabama A & M University, USA
Seifter, Achim, Los Alamos National Laboratory, USA
Sengupta, Deepak, Advance Bio-Photonics, India
Shankar, B. Baliga, General Monitors Transnational, USA
Shearwood, Christopher, Nanyang Technological University, Singapore
Shin, Kyuho, Samsung Advanced Institute of Technology, Korea
Shmaliy, Yuriy, Kharkiv National University of Radio Electronics, Ukraine
Silva Girao, Pedro, Technical University of Lisbon, Portugal
Singh, V. R., National Physical Laboratory, India
Slomovitz, Daniel, UTE, Uruguay
Smith, Martin, Open University, UK
Soleymanpour, Ahmad, Damghan Basic Science University, Iran
Somani, Prakash R., Centre for Materials for Electronics Technol., India
Srinivas, Talabattula, Indian Institute of Science, Bangalore, India
Srivastava, Arvind K., Northwestern University, USA
Stefan-van Staden, Raluca-Ioana, University of Pretoria, South Africa
Sumriddetchka, Sarun, National Electronics and Computer Technology Center, Thailand
Sun, Chengliang, Polytechnic University, Hong-Kong
Sun, Dongming, Jilin University, China
Sun, Junhua, Beijing University of Aeronautics and Astronautics, China
Sun, Zhiqiang, Central South University, China
Suri, C. Raman, Institute of Microbial Technology, India
Sysoev, Victor, Saratov State Technical University, Russia
Szewczyk, Roman, Industrial Research Institute for Automation and Measurement, Poland
Tan, Ooi Kiang, Nanyang Technological University, Singapore,
Tang, Dianping, Southwest University, China
Tang, Jaw-Luen, National Chung Cheng University, Taiwan
Teker, Kasif, Frostburg State University, USA
Thumbavanam Pad, Kartik, Carnegie Mellon University, USA
Tian, Gui Yun, University of Newcastle, UK
Tsiantos, Vassilios, Technological Educational Institute of Kaval, Greece
Tsigara, Anna, National Hellenic Research Foundation, Greece
Twomey, Karen, University College Cork, Ireland
Valente, Antonio, University, Vila Real, - U.T.A.D., Portugal
Vaseashta, Ashok, Marshall University, USA
Vazques, Carmen, Carlos III University in Madrid, Spain
Vieira, Manuela, Instituto Superior de Engenharia de Lisboa, Portugal
Vigna, Benedetto, STMicroelectronics, Italy
Vrba, Radimir, Brno University of Technology, Czech Republic
Wandelt, Barbara, Technical University of Lodz, Poland
Wang, Jiangping, Xi'an Shiyou University, China
Wang, Kedong, Beihang University, China
Wang, Liang, Advanced Micro Devices, USA
Wang, Mi, University of Leeds, UK
Wang, Shinn-Fwu, Ching Yun University, Taiwan
Wang, Wei-Chih, University of Washington, USA
Wang, Wensheng, University of Pennsylvania, USA
Watson, Steven, Center for NanoSpace Technologies Inc., USA
Weiping, Yan, Dalian University of Technology, China
Wells, Stephen, Southern Company Services, USA
Wolkenberg, Andrzej, Institute of Electron Technology, Poland
Woods, R. Clive, Louisiana State University, USA
Wu, DerHo, National Pingtung University of Science and Technology, Taiwan
Wu, Zhaoyang, Hunan University, China
Xiu Tao, Ge, Chuzhou University, China
Xu, Lisheng, The Chinese University of Hong Kong, Hong Kong
Xu, Tao, University of California, Irvine, USA
Yang, Dongfang, National Research Council, Canada
Yang, Wuqiang, The University of Manchester, UK
Ymeti, Aurel, University of Twente, Netherland
Yong Zhao, Northeastern University, China
Yu, Haihu, Wuhan University of Technology, China
Yuan, Yong, Massey University, New Zealand
Yufera Garcia, Alberto, Seville University, Spain
Zagnoni, Michele, University of Southampton, UK
Zeni, Luigi, Second University of Naples, Italy
Zhong, Haoxiang, Henan Normal University, China
Zhang, Minglong, Shanghai University, China
Zhang, Qintao, University of California at Berkeley, USA
Zhang, Weiping, Shanghai Jiao Tong University, China
Zhang, Wenming, Shanghai Jiao Tong University, China
Zhou, Zhi-Gang, Tsinghua University, China
Zorzano, Luis, Universidad de La Rioja, Spain
Zourob, Mohammed, University of Cambridge, UK

Sensors & Transducers Journal (ISSN 1726-5479) is a peer review international journal published monthly online by International Frequency Sensor Association (IFSA). Available in electronic and CD-ROM. Copyright © 2007 by International Frequency Sensor Association. All rights reserved.

Sensors & Transducers Journal

Contents

Volume 98
Issue 11
November 2008

www.sensorsportal.com

ISSN 1726-5479

Research Articles

Nanotechnology-Enabled Sensors: Book Review
S.Y. Yurish………………………………………………………………………………………………….. I

Room Temperature Ammonium Gas Sensing Behavior of Upright-standing ZnO Nano-sheets
Arindam Ghosh , Yuvraj G. Gudage, Ramphal Sharma, Rajaram S. Mane and Sung-Hwan Han 1

Synthesis of Nanocrystalline SnO2 Modified TiO2: a Material for Carbon Monoxide Gas Sensor
A. B. Bodade, M. Alvi, A. V.Kadu, S. V.Jagtap, S. K. Rithe, P. R. Padole and G. N. Chaudhari 6

Glucose Biosensor Based on Electrostatically Functionalized Carbon Nanotubes Bound Glucose Oxidase
Suman, Ashok Kumar, V. K. Jain 16

CO Sensing Properties of Nanostructured $La_{0.8}Sr_{0.2}CoO_3$ Sensors Synthesized by EDTA-Glycol Method
G. N. Chaudhari, A. B. Bodade, S. V. Jagatap, M. J. Pawar 26

Pt/GaN Schottky Diode for Propene (C3H6) Gas Sensing
M. Shafiei, K. Kalantar-Zadeh, M. Kocan, G. Parish, J. Antoszewski, L. Faraone, W. Wlodarski 38

All-digital PLL System for Self-oscillation Mode of Microcantilevers with Integrated Bimorph Actuator and Piezoresistive Readout
Nikolay Nikolov, Nikolay Kenarov, Peycho Popov, Theodor Gotszalk, Ivo Rangelow...................... 45

Modelling of Spring Constant and Pull-down Voltage of Non-uniform RF MEMS Cantilever Incorporating Stress Gradient
Shimul Chandra Saha, Ulrik Hanke, Geir Uri Jensen, Trond Sæther 54

Analysis of a Bimorph Accelerometer Using Analytical and Finite Element Modeling
Hou Xiaoyan. 69

Design of a High Performance MEMS Pressure Sensor Array with Signal Conditioning Unit for Oceanographic Applications
C. RoyChaudhuri, V. Natarajan, P. Chatterjee, S. Gangopadhyay, V. Sreeramamurthy, H. Saha ... 83

On the Modeling of an Open Channel MEMS Based Capacitive Flow Sensor
Vafaghi Maryam, Besharat Sina, Rezazadeh Ghader, Motallebi Asadollah 96

Authors are encouraged to submit article in MS Word (doc) and Acrobat (pdf) formats by e-mail: editor@sensorsportal.com
Please visit journal's webpage with preparation instructions: http://www.sensorsportal.com/HTML/DIGEST/Submition.htm

Sensors & Transducers Journal, Vol. 98, Issue 11, November 2008, pp. 54-68

www.sensorsportal.com

Sensors & Transducers

ISSN 1726-5479
© 2008 by IFSA
http://www.sensorsportal.com

Modelling of Spring Constant and Pull-down Voltage of Non-uniform RF MEMS Cantilever Incorporating Stress Gradient

[1]Shimul Chandra SAHA, [2]Ulrik HANKE, [3]Geir Uri JENSEN, [1]Trond SÆTHER

[1]Department of Electronics and Telecommunications (IET), Norwegian University of Science and Technology (NTNU), 7491 Trondheim, Norway

[2]Institute of Microsystems Technology, Vestfold University College, 3103 Tønsberg, Norway

[3] SINTEF ICT, Gaustadalleen 23, 0371 Oslo, Norway

Tel.: +47 735 92784, fax: +47 7359 1441

E-mail: shimul.saha@iet.ntnu.no

Received: 12 June 2008 /Accepted: 17 November 2008 /Published: 30 November 2008

Abstract: We have presented a model for spring constant and pull-down voltage of a non-uniform radio frequency microelectromechanical systems (RF MEMS) cantilever that works on electrostatic actuation. The residual stress gradient in the beam material that may arise during the fabrication process is also considered in the model. Using basic force deflection calculation of the suspended beam, a stand-alone model for the spring constant and pull-down voltage of the non-uniform cantilever is developed. To compare the model, simulation is performed using standard Finite Element Method (FEM) analysis tolls from CoventorWare. The model matches very well with the FEM simulation results. The model will offer an efficient means of design, analysis, and optimization of RF MEMS cantilever switches. *Copyright © 2008 IFSA.*

Keywords: Modelling, Non-uniform cantilever, Spring constant, Stress gradient, Pull-down voltage

---

1. Introduction

MEMS technology is on the verge of revolutionizing high-frequency applications. Present and future radio frequency (RF) systems require lower weight, volume, cost, and power consumption, especially in portable devices and satellite communications. The system also demands increased functionality and frequency of operation. Reconfiguration is another important issue for the present RF system as they

work in different operating standards and frequency bands. RF MEMS can address these requirements very efficiently. RF MEMS consume very little power (μW). They have a very high cut-off frequency (up to 40 THz) compared with their counterpart PiN diode and FET switches. They have very low insertion loss and high isolation over a wide frequency range from 0 to 100 GHz. The bias circuitry is also much simpler compared with the FET and PIN diode switches. MEMS switches use the same principle as the simple mechanical moving switch, like basic single pole single through (SPST). The beam moves mechanically when actuated, either to make an open or short circuit. Electrostatic actuation is one of the most common actuation mechanisms for MEMS switch. A beam (bridge or cantilever) is suspended from the anchor with actuation electrode placed underneath the beam. A dielectric is used on top of the actuation electrode. For capacitive contact switch the actuation electrode can be used for the contact. For DC contact switch, a separate contact point is used than the actuation electrode. When a DC voltage is applied between the beam and the actuation electrode, an electrostatic force is developed which pulls the beam downward. The DC actuation voltage, at which the beam fully collapses to downstate, is called the pull-down voltage.

Compared with the solid state switching device, RF MEMS switches require higher actuation voltages. Techniques like folded spring and narrower beam close to the anchor than actuation (electrode) area are used to reduce the pull-down voltage [1]. A non-uniform beam, with wider section at actuation and narrower section close to the anchor will have a lower spring constant compared to a uniform beam and reduce the pull-down voltage. To estimate the pull-down voltage for a MEMS switch, an accurate electro mechanical model for the spring constant of the beam is essential. The spring constant depends on the dimension, position and orientation of the suspended beam and actuation electrode. The pull-down voltage depends on the spring constant, initial gap and actuation electrode dimensions. The model of the spring constant and the pull-down voltage for a uniform beam is presented in various literatures, including [1]. For non-uniform beam, some works have recently been published [2, 3]. In the work presented in [2], the model assumes that the force is concentrated on the tip of the cantilever. Therefore, accuracy strongly depends on the size and position of the actuation electrode. In [3], a comparison of pull-down voltage between a uniform and a non-uniform beam is presented using numerical simulations but it does not present any analytical model. In this paper, we develop a novel analytical model for the spring constant and pull-down voltage for a non-uniform cantilever, taking into account the fact that the force may be distributed along the beam.

During fabrication, a stress gradient can develop in the materials of MEMS cantilever. For a positive stress gradient, the cantilever will buckle up. For a negative stress gradient, the cantilever will buckle down. For a relatively long cantilever with a higher negative stress gradient, the switch can be useless as the tip of the cantilever may already touch the bottom electrode. A slight amount of positive stress gradient or zero amount of stress gradient is desirable for a reliable operation of the MEMS cantilever switch. When a positive stress gradient is present, the cantilever will have varying height from the substrate and the gap between suspended beam and bottom electrode or substrate will increase from the anchor toward the end of the beam. This will certainly increase the pull-down voltage of the beam, as it strongly depends on the initial gap. We have also incorporated the stress gradient effect in the non-uniform beam model. This will make the model more complete and it can thus be used for a more general application.

The model will provide an efficient means for analyzing the spring constant and pull-down voltage of a non-uniform beam, using a simple mathematical program. It will be much faster and simpler compared with the commercially available, traditional 3-D analytical tools. The model of the spring constant and its verification with an ideal case is described in section 2. The model extension for pull-down voltage with stress gradient is described in section 3. The modelled pull-down voltage is compared with CoventorWare analyzer (FEM analysis) simulation result in section 4. The paper is concluded in section 5, followed by an appendix.

2. Modelling of a Spring Constant for a Non-uniform Cantilever

In terms of suspended beam structure, RF MEMS switches can be of two types: fixed-fixed bridge and cantilever. Usually, the spring constant of a cantilever is lower than that of a fixed-fixed bridge, as the bridges are rigidly anchored at both ends and the cantilever is anchored at one end. From a circuit point of view, bridges are more useful in shunt configuration and cantilevers are more useful in series configuration. Depending on electrical configuration of a switch (contact), a cantilever can be of two types: capacitive contact and DC contact. In capacitive contact switch, the actuation electrode can be used as a contact capacitance. In the DC contact switch, the actuation electrode is separated from the DC contact point. In this section, we will present the model for the spring constant of a non-uniform cantilever with a wider section over the electrode at the end of the beam.

The top view of a non-uniform capacitive cantilever is shown in Fig. 1. The width of the beam close to the anchor is 'w' and the width of the beam above the actuation electrode is 'wy,' where 'y' is a constant and it can be $1 \geq y$ or $y \geq 1$. For RF MEMS application, $y \geq 1$ is desired. This will give a higher actuation force compared with a uniform beam. The pull-down voltage will be reduced.

A side view of the non-uniform capacitive cantilever is shown in Fig. 2. Total beam length is 'L', actuation electrode length is 'L_e', and initial gap is 'g_0'. The thickness of the beam is 't'. A distributed force 'q' per unit length is working along the entire electrode. An electrostatic actuation is used to pull down the cantilever. The width of the beam above the actuation area is higher than the rest of the beam as shown in Fig. 1. A side view of the DC contact cantilever is shown in Fig. 3. Here, a separate electrode is used for actuation. The metal-metal contact is formed between the end of the beam and transmission line below. For force deflection analysis, we can use the effective beam length 'L' until the end of the actuation electrode. The rest of the parameters are the same as capacitive contact and the electromechanical analysis of pull-down voltage will be identical.

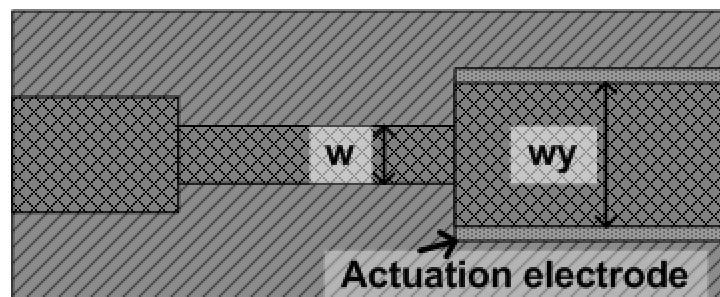

Fig. 1. Top view of a non-uniform capacitive cantilever.

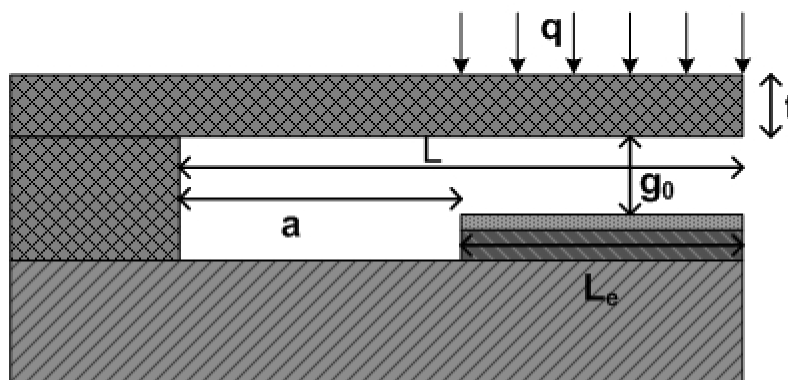

Fig. 2. Side view of a non-uniform capacitive cantilever.

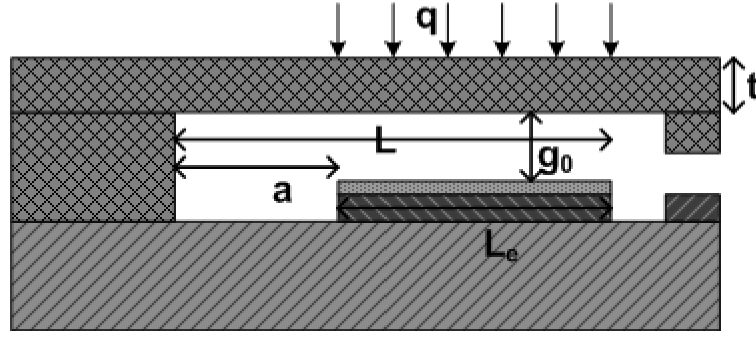

Fig. 3. Side view of a non-uniform DC contact cantilever.

To develop the model, we used the beam diagram with actuation force, moment, and reaction force acting on the beam at different positions. Fig. A1 in the appendix shows such a model. A preliminary model for spring constant and pull-down voltage of the non-uniform cantilever is presented in [4]. The derivation of the spring constant of the non-uniform beam is presented in the appendix, using the Euler-Bernoulli theory [4, 5]. For a force 'q' per unit length, the equation of the deflection '*v*' at any position of the beam from the anchor '*x*' is given by,

$$v = \frac{q}{24EIy}(4Lx^3 - 6L^2x^2 - x^4) + C_3x + C_4 \tag{1}$$

Here 'E' is the Young's modulus of the beam material and 'I' is the moment of inertia and other symbols are as mentioned in Figures 1 and 2. C_3 and C_4 are given by,

$$C_3 = \frac{qaL(a-L)}{2EI}\left(1-\frac{1}{y}\right) + \frac{qa^3}{6EIy} \tag{2}$$

$$C_4 = \frac{qa^2L}{12EI}(3L-4a)\left(1-\frac{1}{y}\right) + \frac{qa^4}{12EI}\left(1+\frac{1}{2y}\right) - \frac{qa^4}{6EIy} \tag{3}$$

For a cantilever, the maximum deflection occurs at the end of the beam or at 'x=L'. The deflection at the end is given by,

$$v_L = -\frac{qL^4}{8EIy} + C_3L + C_4 \tag{4}$$

After replacing the constant and simplification, the maximum deflection of the beam becomes

$$v_L = \frac{-q(L-a)^2(L+a)^2}{8EIy} - \frac{q(L-a)a(a+3L)}{12EI} - \frac{qa^2L}{2EI}(L-a)^2(1-\frac{1}{y}) \tag{5}$$

The spring constant of the cantilever '*k*' is defined, as the ratio of total acting force '*P=q(L-a)*' to the maximum deflection 'v_L' and represented by the equation,

$$k = -\frac{P}{v_L} = -\frac{q(L-a)}{v_L} \tag{6}$$

By inserting equation (5) into equation (6), the spring can be simplified as,

$$k = \frac{24EIy}{3(L-a)(L+a)^2 + 2ya^2(a+3L) + 12aL(L-a)(y-1)} \tag{7}$$

When the beam is uniform, i.e. 'y=1', the expression for '$C_3 = C_{3u}$' and '$C_4 = C_{4u}$' becomes

$$C_{3u} = \frac{qa^3}{6EI} \tag{8}$$

$$C_{4u} = -\frac{qa^4}{24EI} \tag{9}$$

The deflection of the uniform cantilever 'v_u' at any point is given by,

$$v_u = -\frac{q}{24EI}\left[x^4 - 4Lx^3 + 6L^2x^2 - 4a^3x + a^4\right] \tag{10}$$

This matches the expression of deflection in [5]. To test more validity of this expression, we can take some well-known limits in equation (7). If we take the limits 'a=L, a=0, and y=1', we obtain the following spring constants:

$$k \xrightarrow{a=0} \frac{8EIy}{L^3} = \frac{2Ewy}{3}\left(\frac{t}{L}\right)^3 \tag{11}$$

$$k \xrightarrow{a=L} \frac{3EI}{L^3} = \frac{Ew}{4}\left(\frac{t}{L}\right)^3 \tag{12}$$

$$k \xrightarrow{y=1} 2Ewt^3 \frac{L-a}{3L^4 - 4La^3 + a^4} \tag{13}$$

The expressions for spring constants (11)-(13) match the expressions presented in [1, Ch 2].

Using equation (7), we have calculated the variation in spring constant of the cantilever versus the width of the electrode in MathCAD for two different thicknesses. The total beam length is 'L=100 μm' and the electrode length is 'L_e=50 μm'. The thickness 't' of the beam is 1 μm and 2 μm respectively. The width of the beam at the anchor is 'w=50 μm'. The width of the electrode 'wy' is varied from 50 μm to 100 μm ($1 \leq y \leq 2$). Gold is used as material of the cantilever beam. The variation of the spring constant versus the electrode width is shown in Fig. 4.

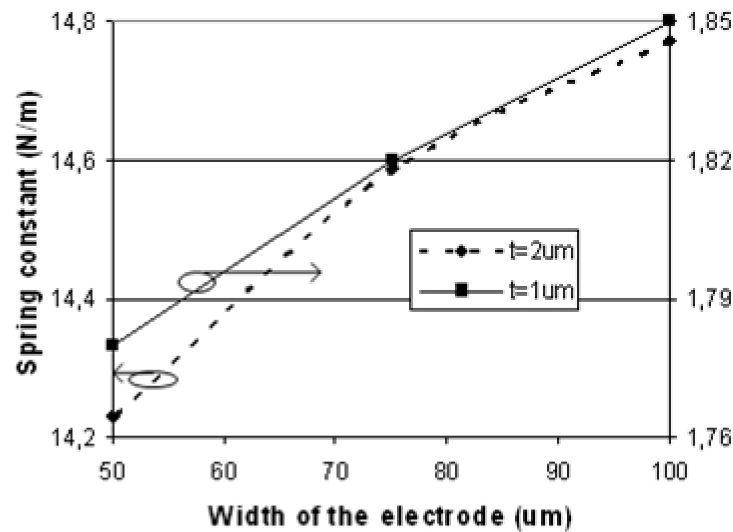

Fig. 4. Variation of spring constant of cantilevers with electrode width.

It can be seen from the Fig. 4 that the spring constant increases to some extent with electrode width, from a uniform beam (i.e., w=50 μm), and it is more prominent for a thicker beam. For a thinner beam, the spring constant is much lower than that for the thicker beam and its spring constant varies very little with electrode width. Also, if the beam is shorter, the spring constant will change more rapidly with electrode width.

3. Pull-down Voltage

3.1. Cantilever without Stress Gradient

For a cantilever switch, with beam width higher than five times of its thickness, the effective Young's modulus is given by [7]

$$E=E^{'}/(1-\upsilon^2)\ , \tag{14}$$

where '$E^{'}$' is the bulk Young's modulus and 'υ' is the poison ratio of the beam material. For majority of the RF MEMS switches, this condition is true. For the beam, with width less than five times its thickness, the effective Young's modulus is equal to the bulk Young's modulus.

When a DC voltage is applied between the suspended beam and actuation electrode the beam moves down due to the electrostatic force. As actuation voltage increases, the electrostatic force increases and the beam moves further down. When the beam moves gradually toward the actuation electrode, for a fixed voltage the electrostatic force increases and the beam moves more downward. The mechanical restoring force due to the spring constant of the beam tries to pull the beam backward. For a particular voltage, when the cantilever maximum deflection becomes equal to one-third of the initial gap, the actuation force becomes higher than the restoring force and the beam collapses. The voltage at which the beam fully collapses to downstate is called pull-down voltage. The pull-down voltage is given by [1, 6],

$$V_p=\sqrt{\frac{8kg_0^3}{27\varepsilon_0 L_e wy}} \tag{15}$$

Here, 'k' is the spring constant, 'g_0' is the initial gap height, 'L_e' is the actuation electrode length, and 'wy' is the actuation electrode width of the cantilever. 'ε_0' is the electrical permittivity of the air.

3.2. Cantilever with Stress Gradient

It is very common to have a stress gradient in the cantilever beam material. The beam may bend up or down due to the stress gradient. A side view of a cantilever with positive stress gradient is shown in Fig. 5. The deflection of the cantilever due to stress gradient only is given by the expression [1, 7]

$$\delta_0(\Gamma) = \frac{\Gamma L^2}{2E}, \tag{16}$$

where 'L' is the beam length and 'Γ' is the stress gradient.

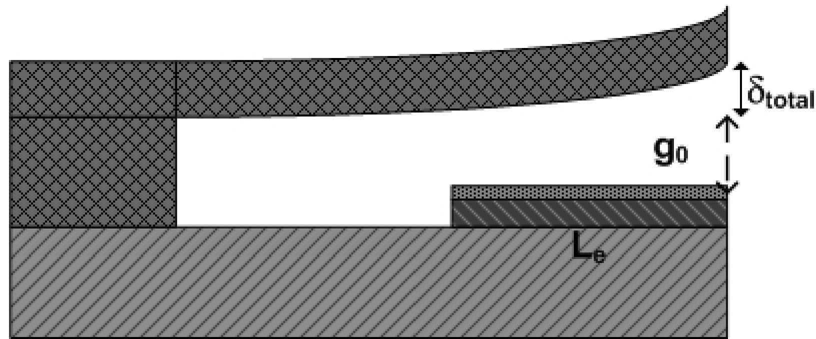

Fig. 5. Side view of a cantilever with positive stress gradient.

The pull-down voltage for a cantilever with stress gradient is given by [7]

$$V_p = \sqrt{\frac{8kg_0(g_0 + \delta_{total})^2}{27\varepsilon_0 L_e wy}}, \tag{17}$$

where 'δ_{total}' is the deflection at the end of the beam and the rest of the symbols are as presented in equation (15).

To verify the model, we have simulated the pull-down voltage of a cantilever with varying stress gradients. The variation in pull-down voltage with stress gradient in CoventorWare analyzer is shown in Fig. 6. Here, the stress gradient factor is a multiplication with a constant stress gradient defined in the simulation. A pull in factor of 8.9 is present for '0' stress gradient factor. From Fig. 6, it can be seen that the pull-down voltage varies linearly with stress gradient factor or stress gradient value. From equation 16, it can be seen that the end tip deflection will increase linearly with the stress gradient. So the total deflection ($g_0+\delta_{total}$) will increase linearly with the stress gradient. From equation 17, we can see that the pull-down voltage will vary linearly with total end tip deflection. So equation 17 is quite accurate for pull-down voltage with stress gradient.

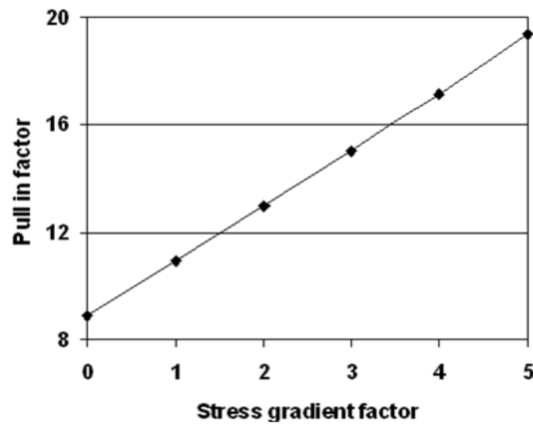

Fig. 6. The pull-down voltage simulation with varying stress gradient.

4. Comparison of the Model with Finite Element Method (FEM) Simulation

We have implemented the analytical expressions in MathCAD to calculate the spring constant and pull-down voltage for cantilever. We have simulated the pull-down voltage of the cantilever using CoventorWare Analyzer to compare results. The simulation for pull-down voltage in CoventorWare is performed both with and without stress gradient. The dimensions of the cantilever are as follows. The length of the cantilever 'L' is 100 µm and 125 µm; the length of the electrode 'L_e' is 50 µm and 75 µm, respectively. The initial gap 'g_0' is 2 µm and the thickness of the cantilever 't' is 1 µm. The beam material is gold with Young's modulus 'E'=79 GPa' and poison ratio 'υ=0.35'. The width of the beam (w) close to the anchor is 50 µm. The electrode width (wy) is varied from 50 µm (uniform) to 100 µm. A cantilever 100 µm long with a thickness of 2 µm is also simulated and compared. The comparison of the pull-down voltage for different widths, lengths, and thicknesses is presented in Table 1. The comparison of the pull-down voltage with and without stress gradient between our model and the CoventorWare analyzer is also shown in Figs. 7–9.

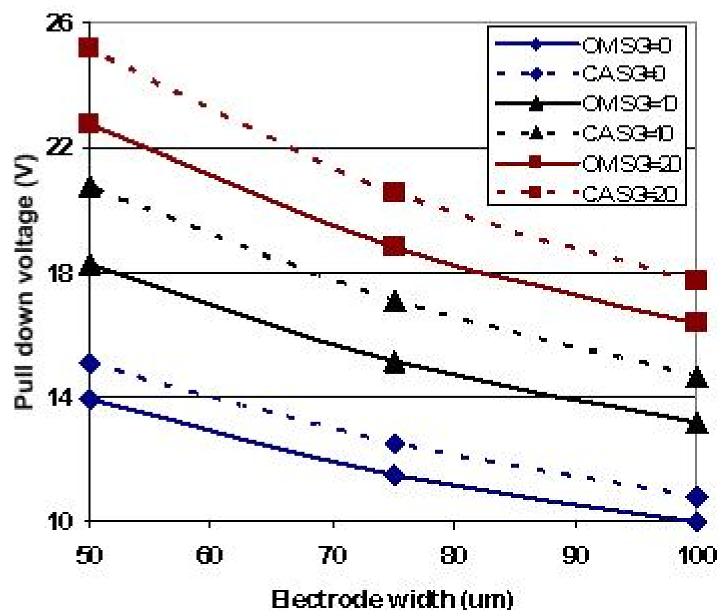

Fig. 7. Comparison of the pull-down voltage with our model and CoventorWare Analyzer simulation result for different electrode width. Total beam length 'L' is 100 µm, beam width 'w' is 50 µm, electrode length 'L_e' is 50 µm, and thickness of the beam 't' is 1 µm. (OM=our model, CA=CoventorWare Analyzer, stress gradients are in MPa/µm).

Table 1. The comparison of pull down voltage of our model with CoventorWare Analyzer. The beam material is gold and the width of the beam close to anchor ‘w’ is 50 µm.

Total beam length ‘L’ (µm)	Electrode Length ‘L_e’ (µm)	Beam thickness ‘t’ (µm)	Electrode width ‘wy’(µm)	Stress gradient ‘Γ’ MPa/µm	Pull down voltage from our Model ‘V_p’ (V)	Pull down voltage from CoventorWare analyzer ‘V_p’ (V)	% of error
100	50	1	50	0	13.90	15.10	8.0
				10	18.30	20.75	12.0
				20	22.75	25.20	9.5
			75	0	11.50	12.50	8.5
				10	15.15	17.10	11.0
				20	18.80	20.60	8.5
			100	0	10.00	10.80	7.0
				10	13.20	14.70	10.0
				20	16.40	17.70	7.0
125	75	1	50	0	8.60	9.50	9.0
				10	12.80	14.10	9.0
				20	17.05	19.20	11.0
			75	0	7.20	7.90	9.0
				10	10.70	11.60	8.0
				20	14.25	15.80	10.0
			100	0	6.30	6.90	8.5
				10	9.40	10.10	7.0
				20	12.50	13.70	8.5
100	50	2	50	0	39.40	42.25	7.0
				10	51.80	56.60	8.5
				20	64.25	71.50	10.0
			75	0	32.50	34.50	6.0
				10	42.80	46.35	7.5
				20	53.10	58.25	8.5
			100	0	28.35	30.15	6.0
				10	37.30	40.10	7.0
				20	46.30	50.25	7.5

From the comparison, it is seen that that the pull-down voltage in the CoventorWare analyzer overestimates around 6–10% from our model for all situations. The percentage of error with a stress gradient is 2–3% higher than without a stress gradient. A few reasons are put forward to explain the overestimation. In our model, it is assumed that the beam will collapse when the beam end moves one-third (666 nm for 2 µm initial gap) of its initial gap. In the CoventorWare Analyzer simulation, it is found that the pull down or collapse of the beam occurs after the beam end moves more than one-third of the initial gap (~800 nm). A simulation of pull-down voltage with beam length ‘L’ 100 µm, electrode length ‘L_e’ 50 µm, beam width ‘w’ 50 µm, electrode width ‘wy’ 75 µm, and thickness ‘t’ of 1 µm is shown in Fig. 10.

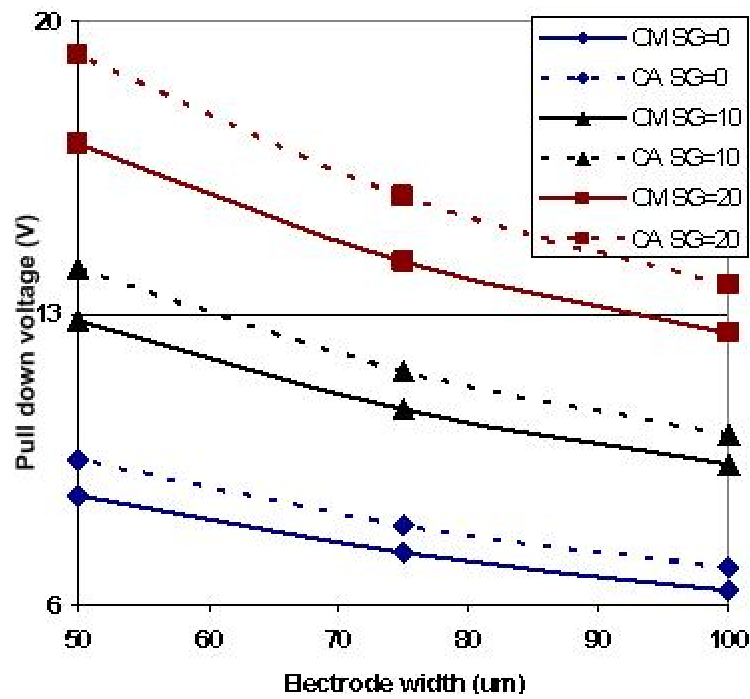

Fig. 8. Comparison of pull-down voltage with our model and CoventorWare Analyzer simulation result for different electrode width. Total beam length 'L' is 125 µm, beam width 'w' is 50 µm, electrode length 'L_e' is 75 µm, and thickness of the beam 't' is 1 µm. (OM=our model, CA=CoventorWare Analyzer, stress gradients are in MPa/µm).

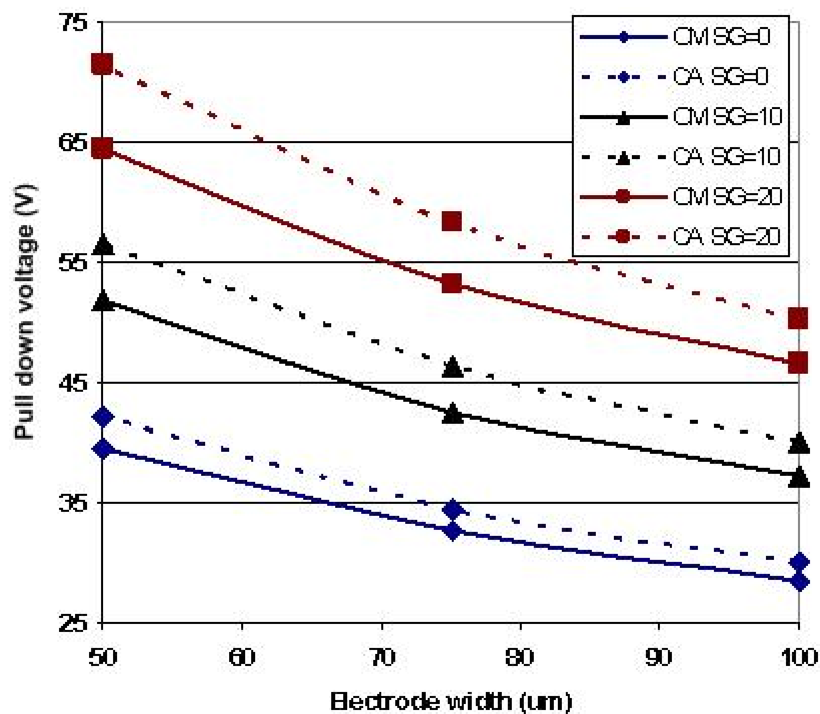

Fig. 9. Comparison of the pull-down voltage with our model and CoventorWare Analyzer simulation result for different electrode width. Total beam length 'L' is 100 µm, beam width 'w' is 50 µm, electrode length 'L' is 50 µm, and thickness of the beam 't' is 2 µm. (OM=our model, CA=CoventorWare Analyzer, stress gradients are in MPa/µm).

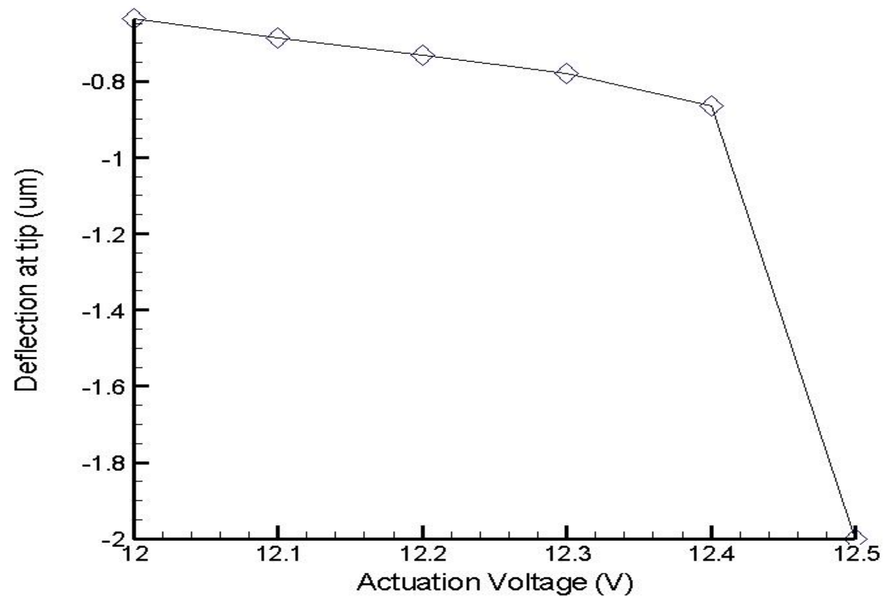

Fig. 10. The deflection of cantilever tip with actuation voltage with 0.1 V increment.

It can be seen form the Fig. 10 that the beam stable position before collapse is 0.85 µm below its initial height. This will cause around 4–5% increase in the pull-down voltage. Pull-down voltage accuracy also depends on the mesh settings. To get a more accurate result, it is always desirable to use very fine mesh. There is a restriction on computer resource and simulation time to use very fine mesh. From CoventorWare tutorial [8], it is found that pull-down voltage decreases with an increased number of mesh elements. We have simulated the pull-down voltage with various mesh sizes. The variation of pull down voltage with an inverse of the number of mesh elements is shown in Fig. 11. Using Rechardson extrapolation [8, page T 4-86] to an infinite number of elements, a 3–4% reduction in the pull-down voltage will occur, from simulated pull down voltage with finer mesh. That means the model that we developed is very accurate.

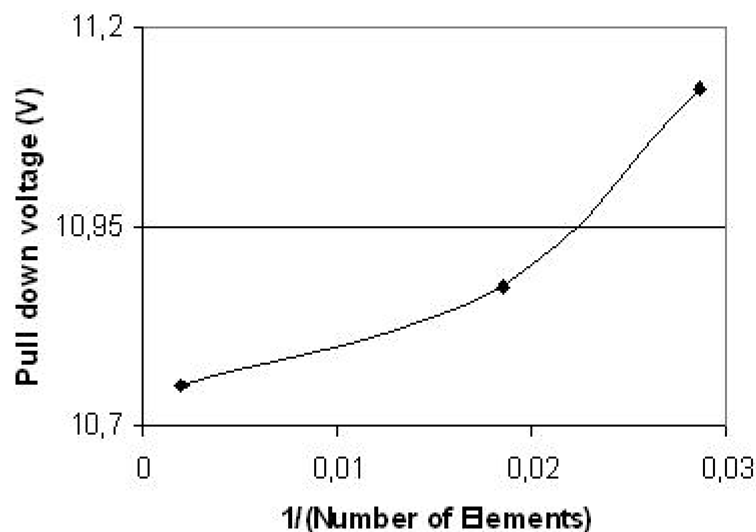

Fig. 11. The variation in pull down voltage with inverse number of mesh elements.

5. Conclusion

We have developed a comprehensive analytical model for spring constant and pull-down voltage of a non-uniform cantilever. The pull-down voltage can also be calculated including stress gradient. We have simulated cantilevers with different lengths and thicknesses in CoventorWare analyzer to compare our model. The model matches quite closely the CoventorWare simulation results in all cases. The ratio between the model and CoventorWare result is almost constant for different electrode widths and lengths. If we scale down the CoventorWare result, considering the extra rigidness and finer mesh, the model will match very closely. This model will be very useful in predicting pull-down voltage of a non-uniform cantilever. It can be implemented using any simple mathematical tools and calculation can be done within a very short time.

Acknowledgement

Authors are grateful to Norwegian Research Council for sponsoring the work through SMiDA project (No 159559/130) and IRRFT project (No 159259/I40).

Reference

[1]. G. M. Rebeiz, RF MEMS Theory, Design and Application, New Jersey, 2nd Edition, *John Wiley and Sons,* 2003.
[2]. S. Afrang and G. Rezazadeh, Design and Simulation of Simple and Varying Section Cantilever and Fixed-Fixed End Types MEMS Switches, in *Proceeding of ICSE 2004*, pp. 593-596.
[3]. L. Lv, Z. Deng, F. Shao, Y. Liu, and K. Han, Analysis and Simulation of RF MEMS for Wireless Communication, in *Proceedings of ISCIT 2005*, pp. 1095-1098.
[4]. S. C. Saha, U. Hanke, G. U. Jensen, and T. Sæther, Modelling of Spring Constant and Pull-down Voltage of Non uniform RF MEMS Cantilever**,** in *Proceedings of 2006 IEEE International Behavioral Modelling and Simulation Conference, San Jose, California, USA,* pp. 56-60.
[5]. J. M. Gere and S. P. Timoshenko, Mechanics of Materials, Boston, 4th Edition, *PSW publication*, 1990.
[6]. J. B. Mauldavin, and G. M. Rebeiz, Nonlinear Electro-Mechanical Modelling of MEMS Switches, *IEEE MTT-S Digest,* 2001, 3, pp. 2119-2122.
[7]. M. Lishchynska, N. Cordero, O. Slattery, and C. O'Mahony, Modelling electrostatic behaviour of microcantilevers incorporating residual stress gradient and non-ideal anchors, *J. Micromech. Microeng.,* 15, 2005, pp. S10-S15.
[8]. CoventorWare Inc 2006.

Appendix

A force moment diagram of the cantilever is shown in Fig. A1.

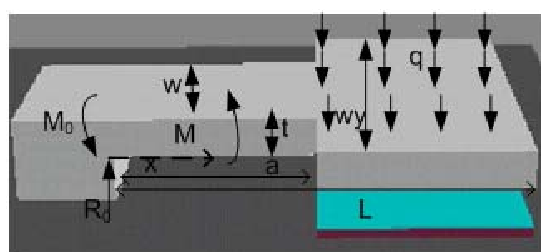

Fig. A1. A force moment diagram of non uniform cantilever.

In Fig. A1, 'L' is the length of the cantilever, 't' is the thickness of the cantilever, 'w' is the width of the cantilever close to the anchor and 'wy' is the width of the cantilever above the actuation electrode region. The distributed force acting on the cantilever electrode is 'q' per unit length. The distance from anchor to start of the actuation electrode is 'a'. The anchor is rigid so a moment of inertia will be applied to keep the cantilever fixed at that position (no vertical movement and rotation). 'M_0' is the moment working at the anchor position. 'R_0' is the reaction forces acting opposite to the actuation force to balance the vertical force [4].

The moment 'M_0' working at the anchor of the cantilever is given by [4],

$$\begin{aligned} M_0 &= q(L-a)\left[a+\frac{L-a}{2}\right] \\ &= \frac{q}{2}(L^2-a^2) \end{aligned} \tag{A1}$$

The vertical force' R_0' working on the anchor is given by,

$$R_0 = q(L-a) \tag{A2}$$

The equation of moment 'M' working on the beam shown in Fig. A1, at the region $0 \le x \le a$, is given by,

$$\begin{aligned} M &= q(L-a)x - \frac{q}{2}(L^2-a^2) \\ EIv'' &= q(L-a)x - \frac{q}{2}(L^2-a^2) \end{aligned} \tag{A3}$$

Here 'x' is distance from the anchor, 'E' is the Young's modulus, 'v''' is the second derivative of deflection, and 'I' is the moment of inertia of the beam in this region and given by, '$I=wt^3/12$'. By integrating equation (A3) in terms of 'x', and simplifying, the first derivative of deflection i.e. the slope of deflection 'v'' is given by,

$$v' = \frac{q}{2EI}\left[(L-a)x^2-(L^2-a^2)x\right]+C_1 \tag{A4}$$

As the anchor is rigid no rotation can take place at the anchor. So at '$x=0$, $v'=0$', which gives '$C_1=0$' from equation (A4). So equation (A4) becomes,

$$v' = \frac{q}{2EI}\left[(L-a)x^2-(L^2-a^2)x\right] \tag{A5}$$

By integrating equation (A5) in terms of 'x' again, we get the equation of deflection 'v' and given by,

$$\begin{aligned} v &= \frac{q}{2EI}\left[(L-a)\frac{x^3}{3}-(L^2-a^2)\frac{x^2}{2}\right]+C_2 \\ &= \frac{qx^2}{12EI}\left[2(L-a)x-3(L^2-a^2)\right]+C_2 \end{aligned} \tag{A6}$$

As the anchor is rigid no vertical movement can occur at that region. At ‘x=0, v=0’, which gives ‘C_2=0’, so the equation of deflection in this region becomes,

$$v = \frac{qx^2}{12EI}\left[2(L-a)x - 3(L^2 - a^2)\right] \tag{A7}$$

For the region a≤x≤L, the equation of moment ‘M’ can be written as,

$$\begin{aligned} M &= q(L-a)x - \frac{q}{2}(L^2 - a^2) - \frac{q}{2}(x-a)^2 \\ \Rightarrow EIyv'' &= qLx - \frac{qL^2}{2} - \frac{q}{2}x^2 \end{aligned} \tag{A8}$$

Here ‘Iy’ is the moment of inertia of the beam above the electrode region, with the width ‘wy’ and thickness ‘t’. By integrating equation (A8),

$$\begin{aligned} EIyv' &= qL\frac{x^2}{2} - \frac{qL^2 x}{2} - \frac{q}{6}x^3 + C_3' \\ v' &= \frac{q}{6EIy}(3Lx^2 - 3L^2 x - x^3) + C_3 \end{aligned} \tag{A9}$$

Using the continuity of the slope of deflection at ‘x=a’, the constant ‘C_3’ is given by.

$$C_3 = \frac{qaL(a-L)}{2EI}\left(1 - \frac{1}{y}\right) + \frac{qa^3}{6EIy} \tag{A10}$$

By integrating the equation (A9) in term of ‘x’ again, the equation for deflection is given by,

$$v = \frac{q}{24EIy}(4Lx^3 - 6L^2x^2 - x^4) + C_3 x + C_4 \tag{A11}$$

By using continuity of deflection at ‘x=a’, ‘C_4’ is given by,

$$C_4 = \frac{qa^2 L}{12EI}(3L - 4a)\left(1 - \frac{1}{y}\right) + \frac{qa^4}{12EI}\left(1 + \frac{1}{2y}\right) - \frac{qa^4}{6EIy} \tag{A12}$$

The maximum deflection of the cantilever occurs at ‘x=L’ or at the end of beam. The deflection at ‘x=L’ from the equation (A11) is given by (without replacing the value of ‘C_3’ and ‘C_4’ for simplification),

$$v_L = -\frac{qL^4}{8EIy} + C_3 L + C_4 \tag{A13}$$

The spring constant of the cantilever ‘k’, ratio of the total applied force ‘q(L-a)’ to the maximum deflection ‘v_L’, is given by,

$$k = -\frac{P}{v_L} = -\frac{q(L-a)}{v_L} \tag{A14}$$

2008 Copyright ©, International Frequency Sensor Association (IFSA). All rights reserved.
(http://www.sensorsportal.com)

Two day IntertechPira conference plus
expert pre-conference workshop

24 - 26 March 2009
Copthorne Tara Hotel, Kensington, London, UK

IMAGE SENSORS
EUROPE 2009

New applications and technology innovations

Don't miss this unrivalled opportunity to find out about the latest developments in technology and applications across the industry!

This year's conference will feature over 20 new presentations from expert analysts and leading integrators from across the supply chain.
Image Sensors Europe 2009 will give you an opportunity to expand your business network as well as learn about trends that matter to your business.

To book now visit www.image-sensors.com or contact Paul Squires on +44 (0)1372 802051 or at paul.squires@pira-international.com

Supported by
PHOTONICS
ADVANCED IMAGING
sensors
EUROPHOTONICS
EDN
IFSA

Get your 20% discount before 2 December 2008!
www.image-sensors.com

Guide for Contributors

Aims and Scope

Sensors & Transducers Journal (ISSN 1726-5479) provides an advanced forum for the science and technology of physical, chemical sensors and biosensors. It publishes state-of-the-art reviews, regular research and application specific papers, short notes, letters to Editor and sensors related books reviews as well as academic, practical and commercial information of interest to its readership. Because it is an open access, peer review international journal, papers rapidly published in *Sensors & Transducers Journal* will receive a very high publicity. The journal is published monthly as twelve issues per annual by International Frequency Association (IFSA). In additional, some special sponsored and conference issues published annually.

Topics Covered

Contributions are invited on all aspects of research, development and application of the science and technology of sensors, transducers and sensor instrumentations. Topics include, but are not restricted to:

- Physical, chemical and biosensors;
- Digital, frequency, period, duty-cycle, time interval, PWM, pulse number output sensors and transducers;
- Theory, principles, effects, design, standardization and modeling;
- Smart sensors and systems;
- Sensor instrumentation;
- Virtual instruments;
- Sensors interfaces, buses and networks;
- Signal processing;
- Frequency (period, duty-cycle)-to-digital converters, ADC;
- Technologies and materials;
- Nanosensors;
- Microsystems;
- Applications.

Submission of papers

Articles should be written in English. Authors are invited to submit by e-mail editor@sensorsportal.com 6-14 pages article (including abstract, illustrations (color or grayscale), photos and references) in both: MS Word (doc) and Acrobat (pdf) formats. Detailed preparation instructions, paper example and template of manuscript are available from the journal's webpage: http://www.sensorsportal.com/HTML/DIGEST/Submition.htm Authors must follow the instructions strictly when submitting their manuscripts.

Advertising Information

Advertising orders and enquires may be sent to sales@sensorsportal.com Please download also our media kit: http://www.sensorsportal.com/DOWNLOADS/Media_Kit_2008.pdf

Springer

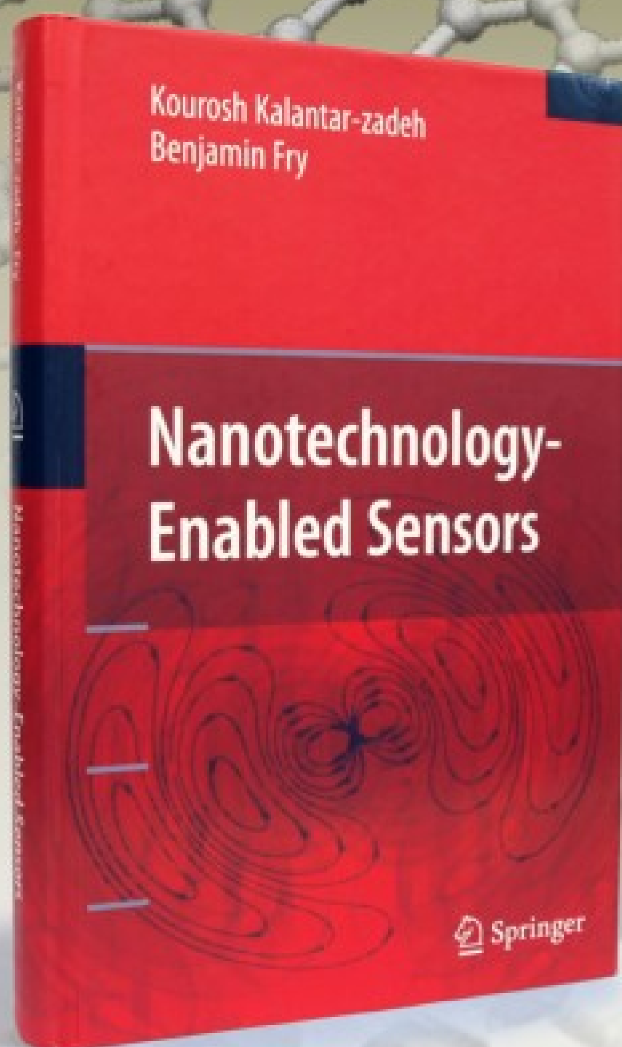

'Nanotechnology-Enabled Sensors is a must have book for researchers as well as graduate students who are either entering these field for the first time, or those alredy conducting research in this multidiscip-linary area and intending to extend their knowledge in the field of nanotechno-logy-enabled sensing.'

Order online:
http://www.sensorsportal.com/HTML/BOOKSTORE/Nanotechnology.htm

www.sensorsportal.com